Antibody-Fc/FcR interaction on macrophages as a mechanism for hyperprogressive disease in non-small cell lung cancer subsequent to PD-1/PD-L1 blockade

(Article begins on next page)

05 November 2024

1 **Antibody-Fc/FcR Interaction on Macrophages as a Mechanism for Hyperprogressive Disease**

2 **in Non-Small Cell Lung Cancer Subsequent to PD-1/PD-L1 Blockade**

3 Giuseppe Lo Russo[1]*, Massimo Moro[2]*, Michele Sommariva[3]*, Valeria Cancila[4]*, Mattia Boeri[2],

4 Giovanni Centonze[2], Simona Ferro[5], Monica Ganzinelli[1], Patrizia Gasparini[2], Veronica Huber[5],

5 Massimo Milione[6], Luca Porcu[7], Claudia Proto[1], Giancarlo Pruneri[6,8], Diego Signorelli[1], Sabina

6 Sangaletti[9], Lucia Sfondrini[3], Chiara Storti[3], Elena Tassi[10,11], Alberto Bardelli[12,13], Silvia

7 Marsoni[12,14], Valter Torri[7], Claudio Tripodo[4], Mario Paolo Colombo[9], Andrea Anichini[10], Licia

8 Rivoltini[5], Andrea Balsari[3#], Gabriella Sozzi[2#§], Marina Chiara Garassino[1#]

9 [1]Thoracic Oncology Unit, Medical Oncology Department 1, Fondazione IRCCS - Istituto Nazionale

10 dei Tumori, Milan (Italy)

11 [2]Tumor Genomics Unit, Department of Research, Fondazione IRCCS - Istituto Nazionale dei

12 Tumori, Milan (Italy)

13 [3]Department of Biomedical Sciences for Health, University of Milan, Milan (Italy)

14 [4]Tumor Immunology Unit, Department of Health Sciences, Human Pathology Section, University

15 of Palermo, Palermo (Italy)

16 [5]Immunotherapy of Human Tumors Unit, Department of Research, Fondazione IRCCS - Istituto

17 Nazionale dei Tumori, Milan (Italy)

18 [6]Department of Pathology and Laboratory Medicine, Fondazione IRCCS - Istituto Nazionale dei

19 Tumori, Milan (Italy)

20 [7]Computational Statistics Unit, Department of Oncology, IRCCS Istituto di Ricerche

21 Farmacologiche Mario Negri, Milano (Italy)

22 [8] Dipartimento di Oncologia ed Emato-Oncologia, University of Milan, Milan (Italy)

23 [9]Molecular Immunology Unit, Department of Research, Fondazione IRCCS - Istituto Nazionale dei

24 Tumori, Milan (Italy)

25 [10]Human Tumors Immunobiology Unit, Department of Research, Fondazione IRCCS - Istituto

26 Nazionale dei Tumori, Milan (Italy)

27 [11]Experimental Hematology Unit, IRCCS San Raffaele Scientific Institute, Milano (Italy)

28 [12]Candiolo Cancer Institute-FPO, IRCCS, Candiolo (Italy)

29 [13] Department of Oncology, University of Torino, Candiolo (Italy);

30 [14]IFOM, Istituto Firc di Oncología Molecolare, Milan Italy

31

32 *These Authors contributed equally at this work

33 [#]These Authors contributed equally at this work as Senior Authors

34 [§] Corresponding author

35

36 **Running title:** ICI induce HP through FcR triggering on macrophages

37 **Keywords:** Hyperprogression; Non-small cell lung cancer; Immune checkpoint inhibitor;

38 macrophages; Fc Receptor;

45

46

47

48

49

2

50 **Corresponding Author:**

51   Dr. Gabriella Sozzi

52 Tumor Genomics Unit, Department of Research,

53 Fondazione IRCCS - Istituto Nazionale dei Tumori,

54 Via Giacomo Venezian 1, 20133 Milan (Italy)

55 Tel. +390223902232; +393480199805

56 Fax. +390223902928

57 e-mail: gabriella.sozzi@istitutotumori.mi.it

58

66 **Body text word count** = 4131 words

67 **Abstract word count** = 249 words

68 **Figures and tables** = 5 (5 Figures, 0 Tables)

69 **Supplementary Data:** 5 (1 Supplementary Materials and Methods, 1 Supplementary Tables, 3

70 Supplementary Figures)

71 **References** = 31

72

ABSTRACT

Background: Hyperprogression (HP), a paradoxical boost in tumor growth, was described in a subset of patients treated with immune checkpoint inhibitors (ICI). Neither clinico-pathological features nor biological mechanisms associated with HP have been identified.

Methods: Among 187 patients with non-small cell lung cancer (NSCLC) treated with ICI at our Institute, cases with HP were identified according to clinical and radiological criteria. Baseline histological samples from patients treated with ICI were evaluated by immunohistochemistry (IHC) for myeloid and lymphoid markers. T-cell deficient mice, injected with human lung cancer cells and patient-derived xenografts (PDXs) belonging to specific mutational subsets, were assessed for tumor growth after treatment with antibodies against mouse and human programmed death receptor-1 (PD-1). The immune microenvironment was evaluated by flow cytometry and IHC.

Results: Among 187 patients, 152 were evaluable for clinical response. We identified 4 categories: 32 cases were defined as Responders (21%), 42 patients with Stable Disease (27.7%), 39 cases defined as Progressors (25.7%) and 39 patients with HP (25.7%). Pre-treatment tissue samples from all patients with HP showed tumor-infiltration by M2-like $CD163^+CD33^+PD\text{-}L1^+$ clustered epithelioid macrophages. Enrichment by tumor-associated macrophages (TAM) was observed, even in tumor nodules from immunodeficient mice injected with human lung cancer cells and with PDXs. In these models, tumor growth was enhanced by treatment with anti-PD-1, but not by anti-PD-1 $F(ab)_2$-fragments.

Conclusions: These results suggest a crucial role of TAM reprogramming, upon Fc receptor engagement by ICI, eventually inducing HP and provide clues on a distinctive immunophenotype potentially able to predict HP.

STATEMENT OF TRANSLATIONAL RELEVANCE

96

97 Hyperprogressive disease in lung cancer and other tumors is an urgent clinical issue reaching 1 out

98 of 5 patients treated with ICI, affecting their prognosis and leading to death in a very short time. As

99 the use of immunotherapy increases in the clinic, it is important to understand the intricacies of this

100 new treatment option in order to optimize treatment approaches. Data already published in the field

101 mainly focused on adaptive immunity without finding any characteristics to predict a priori the

102 phenomenon. Our preclinical findings underline the role of innate immunity in mediating

103 hyperprogression via Fc/FcR triggering on macrophages by anti-PD1 antibody. Accordingly, all

104 patients with HP showed tumor-infiltration by M2-like $CD163^+CD33^+PD\text{-}L1^+$ clustered epithelioid

105 macrophages. These results, pointing to the involvement of innate immune cells in HP, provide new

106 insights into the still unknown mechanisms behind a clinical conundrum.

107

5

INTRODUCTION

The advent of immune checkpoint inhibitors (ICI) has radically changed the paradigm of care for patients with non-small cell lung cancer (NSCLC). Several agents are now approved in the treatment of NSCLC based on their superiority over chemotherapy (1,2). Immunotherapy with antibodies targeting either the programmed death receptor 1 (PD-1) or its ligand (PD-L1) may provide long-term benefits in approximately 20% of patients (2). However, in a subset of patients, ICI paradoxically accelerates tumor growth, a phenomenon known as hyperprogression (HP) (3–6). Studies have estimated that the prevalence of HP in patients with different cancer histotypes treated with ICI may range between 9% and 29% (3–6). No significant histopathological and molecular features capable of predicting *a priori* HP have been identified, with the partial exception of rare *MDM2* amplification and epidermal growth factor receptor (*EGFR*) mutations (5). These observations have ignited an international debate regarding whether HP is a true phenomenon or only representative of a subset of patients with a particularly worse prognosis.

In the tumor microenvironment, the effector functions of innate immune cells may be blunted by the PD-1 receptor, as observed for T lymphocytes, suggesting that these innate cells are another potential target for ICI (7–9). Accordingly, it has been demonstrated that anti-PD-1 antibody can exert antitumor activity in immunodeficient mice via natural killer (NK) cells (8). Conversely, it has been demonstrated that, in PD-1$^{-/-}$ NK cells or in NK cells pre-treated with anti-PD-1 antibody, the production of lytic molecules such as perforins and granzymes is decreased (10). Moreover, tumor-infiltrating dendritic cells (9) and monocytes (11) are reported to release the immunosuppressive cytokine interleukin-10 upon anti-PD-1 treatment. Therefore, it is possible to hypothesize that in some circumstances, PD-1 blockade might exacerbate immunosuppression upon interaction with innate immune cells.

The aim of this study was to investigate, at the clinical and pathological level, the phenomenon of HP in NSCLC patients and to evaluate the role of innate immunity during ICI treatment. To

6

133   eliminate the interference of T lymphocytes we exploited cell lines and patient derived xenografts

134   (PDXs) transplanted in immunodeficient mice.

135

136 **MATERIAL AND METHODS**

137 **Clinical Series**

138 Medical records, radiological findings, and available tumor specimens were collected from patients

139 with NSCLC treated with ICI at the Thoracic Unit of the Istituto Nazionale dei Tumori, Milan,

140 Italy, from July 2013 to December 2017.The study complied with the Declaration of Helsinki and

141 was done in accordance with good clinical practice guidelines. All samples were obtained according

142 to the Internal Review and the Ethics Boards of the Istituto Nazionale Tumori of Milan and all

143 patients provided informed consent. All experimental protocols were approved by the Ethics Boards

144 of the Istituto Nazionale Tumori of Milan (Int 22/15). Radiological evaluation (computed

145 tomography scan with or without brain magnetic resonance imaging) was performed at treatment

146 initiation and every 8 weeks thereafter. Considering that criteria to define patients with HP

147 described by previous authors (3-6) are applicable only in advanced lines, our multidisciplinary

148 team (oncologists, pneumologists, radiologists, and thoracic surgeons) created institutional clinical

149 and radiological criteria designed to identify patients with HP also in first line treatment. Patients

150 with HP or those patients defined as P were classified according to predefined criteria as follows: i)

151 Time-to-treatment failure < 2 months (Time to treatment failure is defined as the time from the start

152 of treatment with ICI to ICI discontinuation for any reason, including progression, patient

153 preference, toxicity or death); ii) Increase of $\geq 50\%$ in the sum of target lesions major diameters

154 between baseline and first radiological evaluation; iii) Appearance of at least two new lesions in an

155 organ already involved between baseline and first radiological evaluation; iv) Spread of the disease

156 to a new organ between baseline and first radiological evaluation; v) Clinical deterioration with

157 decrease in ECOG performance status ≥ 2 during the first 2 months of treatment.

158 Patients who fulfilled at least three of the clinical/radiological criteria were defined as exhibiting

159 HP, while patients with RECIST 1.1 progressive disease as best response without fulfilling at least

160 three criteria were defined as P patients. All R patients and SD patients were classified according to

8

161 their RECIST 1.1 best response. Only patients who underwent at least two cycles of ICI treatment

162 were included in the present analysis.

163

164 **Immunohistochemistry**

165 Immunohistochemistry was carried out on Formal-fixed Paraffin embedded human or PDX tissue

166 sections as described in Supplementary materials and methods. All the slides were analyzed under a

167 Zeiss Axioscope-A1 equipped with fluorescence module and microphotographs were collected

168 using a Zeiss Axiocam 503 Color with the Zen 2.0 Software (Zeiss, Oberkochen DE). All markers

169 were scored according to the percentage of immunoreactive cells out of the total cellularity.

170

171 **Animals Studies**

172 All xenograft experiments were undertaken using 8- to 9-week-old female athymic nude or SCID

173 mice (Charles River Laboratories, Calco, Italy). Human NSCLC cell line H460 tumor-bearing

174 athymic nude mice were treated i.p. or peri-tumorally (p.t.) with either 200 μg of monoclonal

175 antibody anti-mouse PD-1 (clone RMP1-14, BioXCell) or saline, and with either p.t. anti-PD-1

176 $F(ab)_2$ or isotype control. Experiments were carried out in groups of four SCID mice, bearing a

177 PDX sample or a cell suspension (10^5 cells for H460 and PC9 xenograft experiments) in each flank.

178 Mice were treated twice weekly with an i.p. injection of 10 mg/kg Nivolumab (Opdivo, Bristol-

179 Myers Squibb) or Nivolumab $F(ab)_2$ fragments. Mice were maintained in the Animal Facility of the

180 Fondazione IRCCS Istituto Nazionale dei Tumori. Animal experiments were authorized by the

181 Institutional Animal Welfare Body and the Italian Ministry of Health, and performed in accordance

182 with National law (D.lgs 26/2014) and Guidelines for the Welfare of Animals in Experimental

183 Neoplasia (12). At the end of each experiment, tumors were harvested for subsequent analyses.

184

185 **Statistical Analysis**

9

186 Distribution of continuous and categorical biomarkers was summarized by the median as a measure

187 of central tendency and absolute frequencies, respectively. The Cochran–Mantel–Haenszel chi-

188 square test was used to detect statistical association (i.e. $P < 0.05$) in univariate analysis. The

189 median and interquartile range (IQR), follow up was estimated using the reverse Kaplan-Meier

190 method.

191

192 **RESULTS**

193 **Clinical and Pathological Evidence in Patients with Advanced NSCLC Treated with ICI**

194 From July 2013 to December 2017, 187 patients with advanced NSCLC received treatment with ICI

195 at the Thoracic Unit of the Medical Oncology Department at the Istituto Nazionale dei Tumori,

196 Milan, Italy, and 152 patients were evaluable for response. We identified 4 categories: Responders

197 (R, 32 cases, 21%), patients with Stable Disease (SD, 42 cases, 27.7%), Progressors (P, 39

198 cases,25.7%), and patients with HP (39 cases, 25.7%). Patients' characteristics are described in

199 Supplementary Table S1. In this population, after a median follow-up of 32.7 (IQR 15.1-39.6)

200 months, 108 out of 152 patients (71%) died. Median (95% CI) Overall Survival (OS) in the overall

201 population was 11.9 (95% CI 8.8-15.5) months.

202 If we restrict the analysis to patients with HP, median OS significantly decreased to 4.4 (95% CI

203 3.4-5.4) months as compared to 17.7 (95%CI 13.4 -24.1) in non HP patients. Median OS was 8.7

204 (95% CI 5.3-13.4), 17.7 (95% CI 12.7-25.5) and not reached in P, SD and R patients, respectively.

205 Supplementary Table S2 shows the differences between P and HP according to our criteria

206 described in the Materials and Methods section. Of 187 patients, 64 were diagnosed in other centers

207 and could not be included in the present histopathological and molecular analysis. Of the remaining

208 123, 35 patients (11 with HP and 24 without HP) were evaluable for response and had tissue

209 samples suitable for a wide immunohistochemical characterization and gene expression analysis.

210 Patients' characteristics of the extensively analyzed 35 samples resembles the clinical

211 characteristics of the whole treated population

212 Immunohistochemical analysis was performed to assess the presence and distribution of tumor-

213 infiltrating immune elements. The immunophenotype of 11 patients with HP was compared to that

214 of 24 patients without HP (6 P, 11 SD and 7 R). No significant differences were observed among all

215 the clinical classes of patient with respect to the subsets of tumor-infiltrating T lymphocytes (TILs),

216 evaluated by the density of $CD3^+$, $CD4^+$, and $CD8^+$ lymphocytes and $FOXP3^+$ regulatory T cells

217 (Tregs). In addition, no differences were detected between classes of patient in the numbers of

11

218   CD138$^+$ plasma cells (PCs), CD123$^+$ plasmacytoid dendritic cells (pDCs), peritumoral and stromal

219   myeloperoxidase (MPO)$^+$ myeloid cells, CD163$^+$ macrophages, CD33$^+$, PD-1 and PD-L1$^+$ immune

220   cells. However, MPO$^+$ myeloid cells within the tumor were directly correlated ($P=$ 0.0497) and PD-

221   L1 expression in tumor cells was inversely correlated ($P=$ 0.0457) with HP. Furthermore, a

222   statistical trend was shown for the M2 macrophage/myeloid derived suppressor cells marker,

223   Arginase-A I (ArgI) on peritumoral immune cells ($P =$0.0666) (Supplementary Table S3).

224   Gene expression profile (GEP) analysis of pre-treatment tumors did not show any relevant features

225   except for under-expression of pathways related to proliferative activity and cell metabolism in

226   patients experiencing HP after ICI (Supplementary Figures S1A and S1B). The analyses of selected

227   genes representative of immune subsets by RT-qPCR revealed overexpression of the *CD274* gene,

228   encoding for PD-L1, as the only significant marker in R patients (Supplementary Figure S1C).

229   Fluorescence in situ hybridization of *MDM2* and *MDM4* genes, carried out on in a cohort of 30

230   FFPE NSCLC tissue derived from 11 patients with HP and 17 patients without HP, revealed the

231   presence of 3 amplified tumors (2 *MDM2*, 1 *MDM4*) in patients with HP and 6 amplified tumors (4

232   *MDM2*, 1 *MDM4* and 1 *MDM2* and *MDM4*) in patients without HP (Supplementary Figure S2).

233   Notably, we noticed that, in some cases, CD163$^+$ tumor-infiltrating macrophages showed

234   epithelioid morphology (alveolar macrophage-like) with the tendency to form dense clusters within

235   neoplastic foci (Figure 1A). In these cases, the same cells were found to co-express CD33 and PD-

236   L1 (Figure 1B and Figure 2). Such a peculiar morphology, aggregation, and immunophenotype

237   (CD163$^+$CD33$^+$PD-L1$^+$) of macrophages, which we define "complete immunophenotype", was

238   observed in all patients with HP and found to be statistically significant versus patients without HP

239   (P<0.0001) (Supplementary Tables S4 and S5). This complete immunophenotype was also

240   observed in one P patient, two patients with SD, and one R patient (Supplementary Table S5). All

241   other cases experiencing treatment response with stable or slowly progressive disease either lacked

242   the presence of epithelioid macrophages or showed loose clustering, or lacked some of the above

243   markers (mainly CD33$^-$ and/or PD-L1) (Figure 1C and 1D).

12

Anti Mouse PD-1 Antibody Induces Tumor Progression in Athymic Mice

Histopathological analyses showed the presence of clustered $CD163^+CD33^+PD-L1^+$ epithelioid macrophages as a distinctive trait in tumors with HP. Therefore, we sought to test whether macrophages are involved in the detrimental effects associated with anti-PD-1 therapy in preclinical models. Athymic nude mice implanted with human H460 NSCLC cell line were treated either intraperitoneally (i.p.) (Figure 3A) or peritumorally (p.t.) (Figure 3B) with anti-PD-1 antibody (clone RMP1-14) or saline. Anti-PD-1 treatment increased tumor growth compared with the control group, regardless of route and schedule of treatment (Figure 3A and 3B). Anti-PD-1 treatment was also associated with a significant increase in $CD45^+$ leukocyte infiltration at the host–tumor interface, evaluated by immunohistochemistry (IHC) (Figure 3C). Such an increase was mainly due to increasing numbers of intratumoral macrophages ($F4/80^+$ cells) and Arginase-I$^+$-expressing cells, whereas the density of B lymphocytes ($CD45R/B220^+$), granulocytes ($Gr-1^+$) and NK ($NKp46^+$) cells was comparable to the control group (Figure 3C). Of note, Arginase-I was also consistently expressed by the complete immunophenotype intra-tumor macrophages characterizing patients with HP (Figure 1E). Tumor-associated macrophages (TAMs) can express PD-1 and the blocking of this receptor restores antitumor functions (7). Thus, the detrimental boost in tumor growth may not be ascribed to such receptor blockade, but rather to the Fc domain of the antibody which is reported to modulate anti-PD-1 antibody functional activity (13). Accordingly, the same experiments were performed using anti-PD-1 F(ab)$_2$ fragments. The lack of the Fc portion abrogated the increase in tumor growth observed with the whole antibody (Figure 3D).

Anti Human PD-1 Antibody (Nivolumab) Induces Tumor Progression of PDXs in SCID Mice

To exclude a direct involvement of PD-1 expression in immune cells, we treated severe combined immunodeficient (SCID) mice with anti-human PD-1 (Nivolumab) which does not cross-react with the murine counterpart (Supplementary Figure S3A). Since a link between HP and *EGFR* mutational status has been proposed by Kato et al. (5), we compared two NSCLC PDXs, with and without *EGFR* mutation: PDX302 (P53^{C135Y}, EGFR^{L858R}, KRAS^{WT}, APC^{WT}) versus PDX305

13

270   (P53^{WT}, EGFR^{WT}, KRAS^{G12C}, APC^{R1114L}). On PDXs, before treatment, fluorescence-activated cell

271   sorting (FACS) analysis with human anti-PD1 antibody showed expression of PD-1 receptor on a

272   subset of tumor cells (around 1% PD-1$^+$ cells, Supplementary Figure S3B). In addition, IHC

273   analysis showed that F4/80$^+$ epithelioid/monocytoid elements, aggregated in clusters resembling

274   those identified in patients with HP, were appreciable only in PDX302 (Supplementary Figure

275   S3C).

276   SCID mice carrying subcutaneous PDX302 ($n = 8$), but not PDX305 ($n = 8$), showed a significant

277   increase in tumor growth rate compared with controls following twice weekly treatment with

278   Nivolumab (Figure 4A). FACS analysis in lungs of PDX302 bearers showed increased cancer cell

279   dissemination in Nivolumab-treated mice but not in controls (3.88±1.99% vs. 0.87±0.33%, P =

280   0.0286, respectively) (Figure 4B), whereas no differences were detected in PDX305 bearers (data

281   not shown).

282   FACS analysis was also performed on primary tumors for characterization of different myeloid

283   subsets (CD11b, Ly6G, Ly6C, F4/80) and NK cells (CD49b). In PDX302-bearing mice, an increase

284   in CD11b$^+$F4/80^{high} macrophages was observed in the Nivolumab-treated group versus controls

285   (Supplementary Figure S3D), whereas no significant changes occurred in other immune

286   subpopulations. Accordingly, IHC analysis performed on the same tumors revealed accumulation of

287   macrophages and ArgI$^+$-expressing cells (Figure 4C and Supplementary Figure S3E). Notably, in

288   PDX302 the F4/80$^+$ epithelioid/monocytoid clusters were enriched in Nivolumab-treated tumors

289   (Figure 4C).

290   Overall, these data indicate that, in the *EGFR*-mutated PDX302-bearing mice, Nivolumab triggers a

291   detrimental effect characterized by increased tumor growth, lung dissemination and the accrual of

292   macrophages, most likely M2.

293   To further confirm the detrimental effect induced by Nivolumab in other preclinical models,

294   PDX111 (P53^{C242X}, KRAS^{G12V}, CDKN2A^{E69X}, CTNNB1^{T41I}), PDX220 (wild type for all tested

295   genes), H460 (KRAS^{Q61H}, STK11^{Q37*}), and PC9 (EGFR^{L858R}, EGFR$^{E746\_A750del}$, CDKN2A^{G67V}) were

14

296   xenografted in SCID mice. All tested models showed low levels of PD1-expression on tumor cells

297   (ranging from 0.6 to 4%, Supplementary Figure S3B). As with PDX302, an increase in tumor

298   growth was observed in H460- and PC9-bearing mice after Nivolumab treatment. PDX111 tumors

299   showed a variable response, whereas tumors in PDX220- and PDX305-bearing mice showed no

300   response to Nivolumab (Figure 4D).

301   To reinforce the role of the Fc domain of the antibody in boosting tumor growth, PDX302-bearing

302   SCID mice were treated with Nivolumab-F(ab)$_2$ fragments. No HP-like growth was observed

303   (Figure 4E) whereas in the same experiment mice treated with the entire antibody showed HP-like

304   growth, dissemination to lung (Figure 4F) and regional (iliac) lymph node metastases (Figure 3G).

305   In the group pretreated with clodronate, which reduces F4/80$^+$ macrophages, impaired Nivolumab-

306   induced tumor growth was observed (Figure 4E). The F4/80$^+$ macrophages also stained for CD206

307   that marks M2-like subsets and aggregated in fibrotic-like areas in Nivolumab- but not in

308   Nivolumab F(ab)$_2$-treated tumors. In the latter less fibrotic areas than in control mice were observed

309   (Figure 4H).

310   These results suggest that HP is sustained by Nivolumab interaction with M2-like macrophages,

311   most likely via Fc-Fcγ receptor binding (Figure 5).

312

15

DISCUSSION

313 Although ICI have changed the paradigm of care for patients with NSCLC, an in-depth examination

314 of the Kaplan-Meier curves from the CheckMate-026 (14), CheckMate-057 (15), CheckMate-227

315 (16), and KEYNOTE-042 (17) trials showed an excess of disease progression and death in the

316 immunotherapy treatment arms compared with chemotherapy in the first 3 months of treatment.

317 This was also underscored by the European Medicines Agency in response to the appraisal for the

318 second-line use of Nivolumab in non-squamous histologies

319 (http://www.ema.europa.eu/docs/en_GB/document_library/EPAR_-

320 _Product_Information/human/003985/WC500189765.pdf). Furthermore, the benefit of ICI in trials

321 conducted in never smokers and in patients with *EGFR* mutation-positive or Anaplastic Lymphoma

322 Kinase (*ALK*)-mutation-positive NSCLC seems unclear (1,2,5,14,15). The four most important

323 papers on the HP topic showed prevalence rates ranging from 9% to 29% throughout tumor types,

324 including NSCLC (3–6). In all these papers, the ratio of the tumor growth rates before and during

325 ICI treatment was used to identify HP, although with slightly different cut-offs. None of these

326 studies defined pathological features able to predict HP, although *MDM2/4* amplification and *EGFR*

327 alterations were proposed to be associated (5). However, we did not find any significant difference

328 in the frequency of *MDM2/4* amplification between patients with and without HP, and the role of

329 *EGFR* cannot be discussed due to the low number of *EGFR*-mutated patients included in our case

330 series (Supplementary Table S1)

331 Our definition of HP is different from that used in the above-mentioned studies, where radiological

332 imaging before, at the start and after ICI is needed to identify HP. However, in clinical practice all

333 these radiological evaluations are often unavailable, and as a consequence, the criteria used in

334 literature are unable to classify patients with HP considering that ICI are starting to be widely used

335 as first line therapy. Furthermore, both Response Evaluation Criteria In Solid Tumors (RECIST) 1.1

336 and Immune-related Response Evaluation Criteria In Solid Tumors (irRECIST) criteria, used in the

16

338 reported analyses, considered only changes in tumor size and did not take into account non-target

339 lesions, such as lymphangitis and pathological lesions under 10 mm. In addition, functional and

340 clinical aspects, such as deterioration in performance status, were not considered. Therefore, we

341 decided to include both clinical and radiological criteria to identify patients with HP in our series.

342 These proposed criteria might overestimate the real fraction of patients experiencing HP; for these

343 reasons, a clinical trial is ongoing within our Institute to properly validate the criteria and thereby

344 obtain the true rate of HP as well as the distinctive immunophenotype.

345 Nivolumab-treated cell lines and PDX-bearing SCID mice mirrored the clinical observation of HP

346 following treatment with ICI. Interestingly, patients and mice classified with HP share a similar

347 tumor immunophenotype. Indeed, the population of $F4/80^+CD206^+Arginase-A1^+$ cells emerging

348 from PDXs with HP matches macrophage features of the human counterpart (Figures 1A, 4C, 4H

349 and Supplementary Figure S3C). M2-like macrophages were preferentially associated with fibrotic

350 foci in PDXs that experience HP-like tumor growth after PD-1 blockade. The recruitment of these

351 myeloid cells may promote a peculiar cancer-associated innate response that may affect tumor

352 growth. Indeed, Knipper at al. described a cross-talk between myeloid cells and fibroblasts

353 promoting skin fibrosis that could provide proliferative and pro-survival signals in cancer cells (18).

354 Prominent mitotic figures can be consistently identified in Nivolumab-treated tumor foci embedded

355 in a fibrotic stroma. In human samples, the accumulation of these cells is apparently unrelated to the

356 extent and distribution of tumor-infiltrating T-cell populations.

357 The role of the innate immune system in mediating the effects of ICI is now clearly emerging. Cells

358 of myeloid origin present in the tumor microenvironment decrease the effects of ICI via PD-L1

359 expression (19), by "stealing" anti-PD-1 antibody from the membrane of T lymphocytes that return

360 to anergy (20) or by secreting immunosuppressive molecules (21). Our study provides novel

361 evidence of negative immuno-regulatory role exerted by $PD-L1^+$ macrophages enriched at tumor

362 site under treatment with ICI. Pre-treatment lesions from all patients classified as HP showed tumor

363 infiltration by clustered epithelioid macrophages characterized by a $CD163^+CD33^+PD-L1^+$ profile.

17

364   Interestingly, CD163$^+$ PD-L1$^+$ macrophages represent a common immune landscape for different

365   tumors. PD-L1$^+$ macrophages have been recently described to accumulate in tight clusters at the

366   tumor invasive margin in NSCLC (22). Macrophages expressing both PD-L1 and the "M2" marker

367   CD163 have been described in MSI-colorectal cancer (23), triple-negative breast cancer (24),

368   gastric and cervical cancer (25,26). In some of these studies, the presence of PD-L1$^+$ macrophages

369   has been associated with poor prognosis (24,26) and/or with immunosuppressive function through

370   IL-10 production (27). In addition, the concurrent expression of CD163, CD33, and PD-L1 has been

371   recently described in alveolar macrophages from acute respiratory distress syndrome patients, a non

372   oncological condition present in 10% of subjects admitted to intensive care units (28). In this

373   regard, we observed an increased infiltration of M2 macrophages after anti-PD-1 administration,

374   providing evidence for their involvement in determining HP. TAMs can also express PD-1 that, if

375   neutralized, can restore M1-like properties (7). This likely excludes blockade of PD-1 signaling in

376   our models that remain rather oriented to M2. Therefore, we examined the possibility of FcR

377   engagement as a modulator of anti-PD-1 activities (13). Upon testing the F(ab)$_2$ moiety in

378   comparison to whole Ab, we have shown that Nivolumab without the Fc domain no longer induces

379   HP-like disease in our models.

380   The anti-mouse PD-1 clone RMP1-14, utilized for the treatment of tumor-bearing athymic mice, is

381   a rat immunoglobulin IgG2a reported to interact with the mouse inhibitory receptor, FcγRIIb (13).

382   FcγRIIb has been shown to be involved in dampening the immune response, and impairments in

383   FcγRIIb function are associated with an exacerbation of inflammatory processes (29). The anti-

384   human PD-1 antibody Nivolumab is an IgG4 isotype with reduced binding affinity to activating

385   FcγRs, thereby avoiding antibody-dependent cell-mediated cytotoxicity on PD-1$^+$ immune cells

386   (30). However, Nivolumab maintains the ability to bind to the inhibitory FcγRIIb receptor (13).

387   Therefore, we suggest a possible role of FcγRIIb in the detrimental effect associated with anti-PD-1

388   therapy. However, since both human IgG4 and rat IgG2a can bind at lower affinity to other FcRs,

389   the involvement of these receptors cannot be excluded. Further studies elucidating the involvement

18

390 of FcRs in the development of HP are required. Very recently, a report described PD-1 expression

391 in one NSCLC case with HP and in one mouse NSCLC cell line. The latter treated with anti murine

392 PD-1 Ab underwent accelerated tumor growth (31). This interesting and logical explanation of HP

393 can't be totally supported by the low expression/prevalence of PD-1 on tumors and by $F(ab)_2$

394 experiments in mice. We found clusters of PD-1 expressing cells in 2 out of 11 patients with HP

395 (data not shown) and in all xenografts and PDXs, although at low levels (0.6 - 4%) and with no

396 correlation with HP-like progression.

397 In conclusion, the ongoing debate regarding whether HP is a true phenomenon or only

398 representative of patients with a particularly worse prognosis is confirmed in our preclinical models,

399 where ICI are able to boost tumor growth in a manner akin to the clinical observations of HP in

400 patients with NSCLC. Our results suggest that FcR triggering of clustered epithelioid macrophages

401 with a specific immunophenotype by ICI delivers a signaling cascade that promotes functional

402 reprogramming of these cells toward a more aggressive pro-tumorigenic behavior. This eventually

403 induces HP in a subset of patients with distinctive immune and genetic profiles (depicted in Figure

404 **5**). Our analyses, for the first time, suggest a role of innate immunity in this process. A further

405 prospective validation of the HP immunophenotype and its relationship with specific genotypes, as

406 well as the new proposed clinical criteria to classify HP, is ongoing.

407

19

Authors' Contributions

Conception and design: GS, MCG , ABardelli, SM, LR, AA, ABalsari

Development of methodology: VC, GC, SF, PG, CS

Acquisition of data: CT, MMilione, MB, MS, MMoro, GL, PG, MG, VH, CP, DS, ET, SS

Analysis and interpretation of data: CT, MMoro, MS, GL, GP, LP, VT, CP, DS, LS, SS

Writing, review and/or revision of the manuscript: ABardelli, SM, MS, MMoro, MG CP, DS, GL,
MPC, CT, GA, AA, ABalsari, LR, GS, MCG

Study supervision: MPC, GS, MCG, GA

20

428 **REFERENCES**

429 1. Califano R, Kerr K, Morgan RD, Lo Russo G, Garassino M, Morgillo F, et al. Immune

430   Checkpoint Blockade: A New Era for Non-Small Cell Lung Cancer. Curr Oncol Rep.

431   Current Oncology Reports; 2016;18.

432 2. Assi HI, Kamphorst AO, Moukalled NM, Ramalingam SS. Immune checkpoint inhibitors in

433   advanced non–small cell lung cancer. Cancer. 2018;124:248–61.

434 3. Champiat S, Dercle L, Ammari S, Massard C, Hollebecque A, Postel-Vinay S, et al.

435   Hyperprogressive disease is a new pattern of progression in cancer patients treated by anti-

436   PD-1/PD-L1. Clin Cancer Res. 2017;23:1920–8.

437 4. Saâda-Bouzid E, Defaucheux C, Karabajakian A, Coloma VP, Servois V, Paoletti X, et al.

438   Hyperprogression during anti-PD-1/PD-L1 therapy in patients with recurrent and/or

439   metastatic head and neck squamous cell carcinoma. Ann Oncol Off J Eur Soc Med Oncol.

440   2017;28:1605–11.

441 5. Kato S, Goodman A, Walavalkar V, Barkauskas DA, Sharabi A, Kurzrock R.

442   Hyperprogressors after immunotherapy: Analysis of genomic alterations associated with

443   accelerated growth rate. Clin Cancer Res. 2017;23:4242–50.

444 6. Ferrara R, Caramella C, Texier M, Valette CA, Tessonnier L, Mezquita L, et al.

445   Hyperprogressive disease (HPD) is frequent in non-small cell lung cancer (NSCLC) patients

446   (pts) treated with anti PD1/PD-L1 monoclonal antibodies (IO). Ann Oncol. Oxford

447   University Press; 2017;28:abstract 1306PD.

448 7. Gordon SR, Maute RL, Dulken BW, Hutter G, George BM, McCracken MN, et al. PD-1

449   expression by tumour-associated macrophages inhibits phagocytosis and tumour immunity.

450   Nature. Nature Publishing Group; 2017;545:495–9.

451 8. Liu Y, Cheng Y, Xu Y, Wang Z, Du X, Li C, et al. Increased expression of programmed cell

452   death protein 1 on NK cells inhibits NK-cell-mediated anti-tumor function and indicates poor

453   prognosis in digestive cancers. Oncogene. 2017;36:6143–53.

21

454   9.   Lamichhane P, Karyampudi L, Shreeder B, Krempski J, Bahr D, Daum J, et al. IL10 release

455   upon PD-1 blockade sustains immunosuppression in ovarian cancer. Cancer Res.

456   2017;77:6667–78.

457   10.   Solaymani-Mohammadi S, Lakhdari O, Minev I, Shenouda S, Frey BF, Billeskov R, et al.

458   Lack of the programmed death-1 receptor renders host susceptible to enteric microbial

459   infection through impairing the production of the mucosal natural killer cell effector

460   molecules. J Leukoc Biol [Internet]. 2015;99:2–9.

461   11.   Said EA, Dupuy FP, Trautmann L, Zhang Y, Shi Y, El-Far M, et al. Programmed death-1-

462   induced interleukin-10 production by monocytes impairs CD4 + T cell activation during HIV

463   infection. Nat Med [Internet]. Nature Publishing Group; 2010;16:452–9.

464   12.   Workman P, Aboagye EO, Balkwill F, Balmain A, Bruder G, Chaplin DJ, et al. Guidelines

465   for the welfare and use of animals in cancer research. Br J Cancer. 2010;102:1555–77.12

466   13.   Dahan R, Sega E, Engelhardt J, Selby M, Korman AJ, Ravetch J V. FcγRs Modulate the

467   Anti-tumor Activity of Antibodies Targeting the PD-1/PD-L1 Axis. Cancer Cell. Elsevier;

468   2015;28:285–95.

469   14.   Carbone DP, Reck M, Paz-Ares L, Creelan B, Horn L, Steins M, et al. First-Line Nivolumab

470   in Stage IV or Recurrent Non–Small-Cell Lung Cancer. N Engl J Med. 2017;376:2415–26.

471   15.   Borghaei H, Paz-Ares L, Horn L, Spigel DR, Steins M, Ready NE, et al. Nivolumab versus

472   Docetaxel in Advanced Nonsquamous Non–Small-Cell Lung Cancer. N Engl J Med.

473   2015;373:1627–39.

474   16.   Hellmann MD, Ciuleanu T-E, Pluzanski A, Lee JS, Otterson GA, Audigier-Valette C, et al.

475   Nivolumab plus Ipilimumab in Lung Cancer with a High Tumor Mutational Burden. N Engl

476   J Med [Internet]. 2018;NEJMoa1801946.

477   17.   Lopes G, Wu Y-L, Kudaba I, Kowalski D, Chul Cho B, Castro G, et al. Pembrolizumab

478   (pembro) versus platinum-based chemotherapy (chemo) as first-line therapy for

479   advanced/metastatic NSCLC with a PD-L1 tumor proportion score (TPS) ≥ 1%: Open-label,

22

480   phase 3 KEYNOTE-042 study. J Clin Oncol. 2018;36:suppl. abstr. LBA4.

481   18.   Knipper JA, Willenborg S, Brinckmann J, Bloch W, Maaß T, Wagener R, et al. Interleukin-4

482   Receptor α Signaling in Myeloid Cells Controls Collagen Fibril Assembly in Skin Repair.

483   Immunity. 2015;43:803–16.

484   19.   Antonios JP, Soto H, Everson RG, Moughon D, Orpilla JR, Shin NP, et al.

485   Immunosuppressive tumor-infltrating myeloid cells mediate adaptive immune resistance via

486   a PD-1/PD-L1 mechanism in glioblastoma. Neuro Oncol. 2017;19:796–807.

487   20.   Arlauckas SP, Garris CS, Kohler RH, Kitaoka M, Cuccarese MF, Yang KS, et al. In vivo

488   imaging reveals a tumor-associated macrophage – mediated resistance pathway in anti – PD-

489   1 therapy. Sci Transl Med. 2017;1–10.

490   21.   Marvel D, Gabrilovich DI. Myeloid-derived suppressor cells in the tumor

491   microenvironment : expect the unexpected. J Clin Investig. 2015;125:3356–64.

492   22.   Lavin Y, Kobayashi S, Leader A, Amir E ad D, Elefant N, Bigenwald C, et al. Innate

493   Immune Landscape in Early Lung Adenocarcinoma by Paired Single-Cell Analyses. Cell

494   [Internet]. Elsevier Inc.; 2017;169:750–765.e17.

495   23.   Korehisa S, Oki E, Iimori M, Nakaji Y, Shimokawa M, Saeki H, et al. Clinical significance

496   of programmed cell death-ligand 1 expression and the immune microenvironment at the

497   invasive front of colorectal cancers with high microsatellite instability. Int J Cancer.

498   2018;142:822–32.

499   24.   Adams A, Vail P, Ruiz A, Mollaee M, McCue P, Knudsen E, et al. Composite analysis of

500   immunological and metabolic markers defines novel subtypes of triple negative breast

501   cancer. Mod Pathol. 2018;2:288–98.

502   25.   Harada K, Dong X, Estrella JS, Correa AM, Xu Y, Hofstetter WL, et al. Tumor-associated

503   macrophage infiltration is highly associated with PD-L1 expression in gastric

504   adenocarcinoma. Gastric Cancer. Springer Japan; 2018;21:31–40.

505   26.   Heeren AM, Punt S, Bleeker MC, Gaarenstroom KN, Van Der Velden J, Kenter GG, et al.

23

506   Prognostic effect of different PD-L1 expression patterns in squamous cell carcinoma and

507   adenocarcinoma of the cervix. Mod Pathol [Internet]. Nature Publishing Group;

508   2016;29:753–63.

509 27. Kubota K, Moriyama M, Furukawa S, Rafiul HASM, Maruse Y, Jinno T, et al.

510   CD163+CD204+ tumor-associated macrophages contribute to T cell regulation via

511   interleukin-10 and PD-L1 production in oral squamous cell carcinoma. Sci Rep [Internet].

512   Springer US; 2017;7:1–12.

513 28. Morrell ED, Wiedeman A, Long SA, Gharib SA, West TE, Skerrett SJ, et al. Cytometry TOF

514   identifies alveolar macrophage subtypes in acute respiratory distress syndrome. JCI Insight

515   [Internet]. 2018;3:1–11.

516 29. Roghanian A, Stopforth RJ, Dahal LN, Cragg MS. New revelations from an old receptor:

517   Immunoregulatory functions of the inhibitory Fc gamma receptor, FcγRIIB (CD32B). J

518   Leukoc Biol. 2018;1–12.

519 30. Madorsky Rowdo FP, Baron A, Urrutia M, Mordoh J. Immunotherapy in cancer: A combat

520   between tumors and the immune system; you win some, you lose some. Front Immunol.

521   2015;6:2–13.

522 31. Du S, McCall N, Park K, Guan Q, Fontina P, Ertel A, et al. Blockade of Tumor-Expressed

523   PD-1 promotes lung cancer growth. Oncoimmunology. 2018;

524

525

526

527   **FIGURE LEGENDS**

528   **Figure 1. Immunohistochemical analyses for CD163, PD-L1 and CD33 in representative**

529   **hyperprogressor and non-hyperprogressor cases.**

530   (**A**) Representative microphotographs detailing the presence of macrophages displaying epithelioid

531   morphology and expression of CD163, PD-L1, and CD33 markers (defined as *complete phenotype*)

532   in four hyperprogressor cases. (**B**) Double immunofluorescence staining for CD163 (green) and PD-

533   L1 (red) showing the co-expression of the two markers in epithelioid macrophages (arrows). (**C**)

534   Representative microphotographs detailing the presence of macrophages displaying epithelioid

535   morphology, variable clustering and the incomplete expression of the three CD163, PD-L1, and

536   CD33 markers (defining the complete phenotype of HP patients) in two cases of non-HP patients

537   (stable disease). (**D**) Representative microphotographs detailing the presence of myeloid elements

538   with non-epithelioid morphology (stellate or spindle-shaped cells) on CD163, PD-L1, and CD33

539   markers populating tumor infiltrates of non-HP patients (one stable disease and one response). (**E**)

540   Representative microphotographs relative to Arginase-A1 expression by clustered epithelioid

541   macrophages in four HP patients' infiltrates. Magnification 20x.

542   **Figure 2. CD33, CD163, and PD-L1 co-localization in clustered macrophages with epithelioid**

543   **morphology**

544   Immunofluorescence panels from prototypical hyperprogressive disease infiltrates showing the co-

545   localization of CD33, CD163, and PD-L1 in clustered macrophages with epithelioid morphology.

546   Three different combinations of double-marker stainings are shown. Green signal and red signal

547   correspond to Opal-520 and Opal-620 fluorophores, respectively. Original magnifications x100 and

548   x400.

549   **Figure 3. Anti Mouse PD-1 Antibody Induces Tumor Progression in Athymic Mice**

550   Athymic nude mice were xenografted with H460 lung cancer cell lines and treated i.p. (n=6

551   mice/group) (**A**) or p.t. (n=5 mice/group) (**B**) with 200µg of anti-mouse PD-1 blocking antibody

552   (red dots) or with vehicle (black dots). Red arrows indicate the days of anti-PD-1 antibody

25

553   treatment. Dots represent Mean ± SEM of tumor volume for each group. **P <0.01 by Mixed

554   Models ANOVA. (**C**) Representative immunohistochemistry images and quantification of

555   leukocytes (CD45^{+}), macrophages (F4/80^{+}), Arginase-I^{+}, B lymphocytes (CD45R/B220^{+}),

556   granulocytes (Gr-1^{+}) and NK (NKp46^{+}) cells in the tumor microenvironment of H460 lung cancer

557   xenografts collected from the study illustrated in Figure 2B (p.t. experiment, n=5 mice/group).

558   Original magnification x20. *P <0.05, **P <0.01 by Mann-Whitney U test. (**D**) Athymic nude mice

559   were xenografted with H460 lung cancer cell lines and treated i.p. with 200 µg anti-PD-1 F(ab)$_2$

560   (blue dots) or with vehicle (black dots) (n=6 mice/group). Blue arrows indicate the days of anti-PD-

561   1 antibody treatment. Dots represent Mean ± SEM of tumor volume for each group.

562   **Figure 4. Anti Human PD-1 Antibody (Nivolumab) Induces Tumor Progression of PDXs in**

563   **SCID Mice**

564   (A) PDX302 (P53C135Y, EGFRL858R, KRASWT, APCWT) and PDX305 (P53WT, EGFRWT,

565   KRASG13C, APCR1114L) samples were injected in both flanks of SCID mice (n = 4). Mice were

566   treated with 10 mg/kg i.p. Nivolumab (red dots) twice weekly from day 1 after tumor implant to the

567   end of the experiment. **P < 0.01 by mixed models ANOVA. (B) Analysis of tumor cells

568   disseminated to mice lungs. Mice lungs were analyzed by FACS, after tissue dissociation to single

569   cells, for the presence of human disseminated cells. Graphs indicate the percentage of human cells

570   in Nivolumab treated and control mouse lungs. *P < 0.05 (C) Representative images showing

571   F4/80+ cells with epithelioid/monocytoid elements aggregated in clusters in an untreated PDX302

572   model. (D) Dot plot summarizing the results of the effects of Nivolumab treatment in all tested

573   PDX (PDX302, PDX305, PDX111, and PDX220) and xenograft models (H460 and PC9).

574   Response rate was estimated as described in the Materials and Methods section. (E) PDX302

575   (P53C135Y, EGFRL858R, KRASWT, APCWT) samples were injected in both flanks of SCID

576   mice (n = 4). Mice were treated with 10 mg/kg i.p. Nivolumab, Nivolumab F(ab)2 or clodronate

577   plus Nivolumab twice weekly (once weekly for clodronate injection) from day 1 after tumor

578   implant to the end of the experiment. *P < 0.05. (F) Analysis of tumor cells disseminated to mice

26

579   lungs. Mice lungs were analyzed by FACS, after tissue dissociation to single cells, for the presence

580   of human disseminated cells. Graphs indicates the percentage of human cells in Nivolumab-,

581   Nivolumab F(ab)$_2$- or Clodronate plus Nivolumab treated and control mouse lungs. *P < 0.05

582   compared to control; #P < 0.05 compared to Nivolumab-treated (G) Representative IHC images of

583   mouse iliac lymph nodes show tumor cell dissemination with the presence of a metastatic nodule

584   (indicated by the asterisk) only in Nivolumab-treated mice (H/E: hematoxylin/eosin staining; CK:

585   pan-cytokeratin staining). (H) H&E and Masson's trichrome staining showing the presence of

586   fibrotic areas with consistent matrix deposition in Untreated, Nivolumab- and Nivolumab F(ab)$_2$-

587   treated representative cases. IHC analysis for CD206$^+$ macrophages highlighting the enrichment in

588   macrophages in Nivolumab treated tumor.

589

590   **Figure 5. Hypothesized mechanism through which macrophages and ICI are involved in**
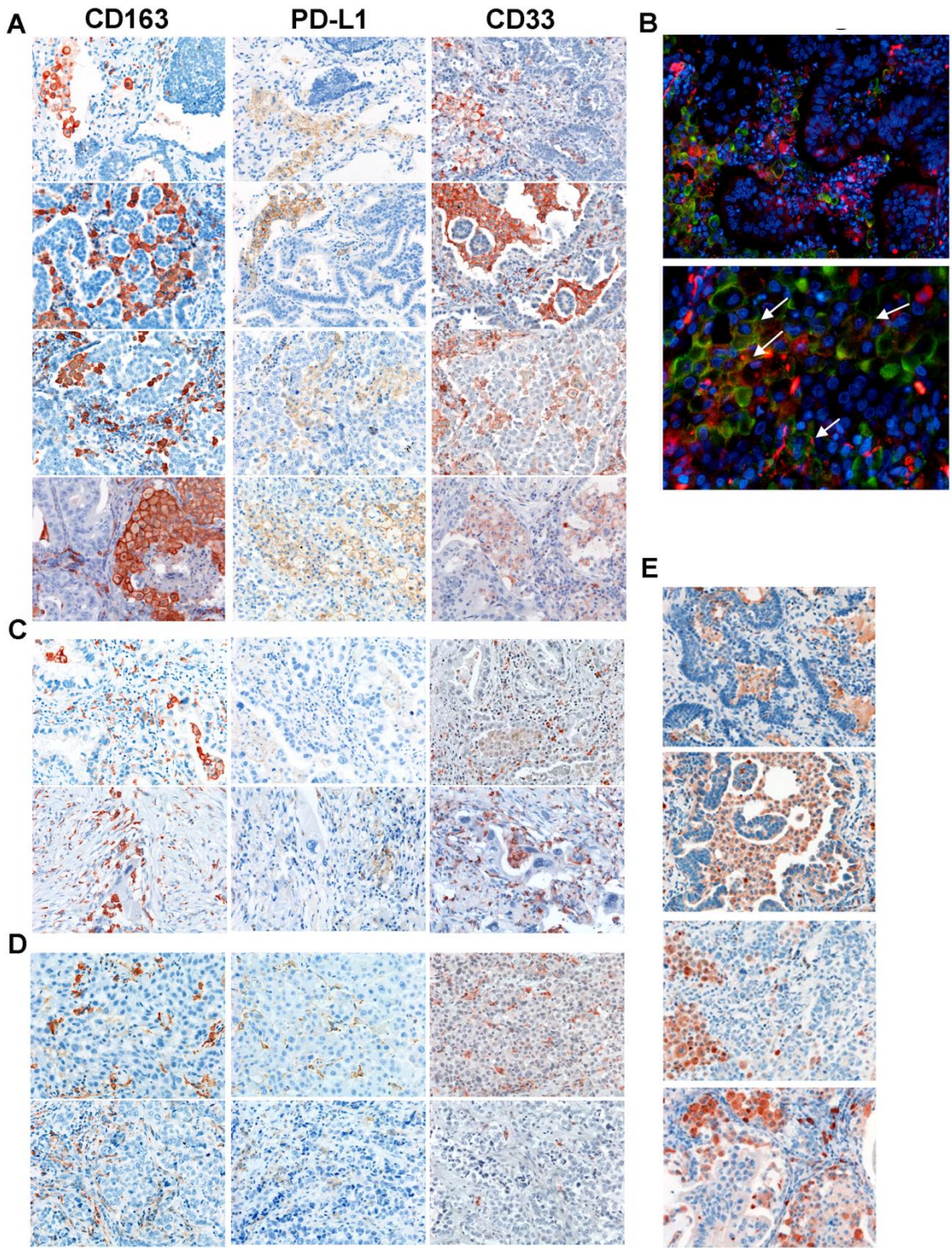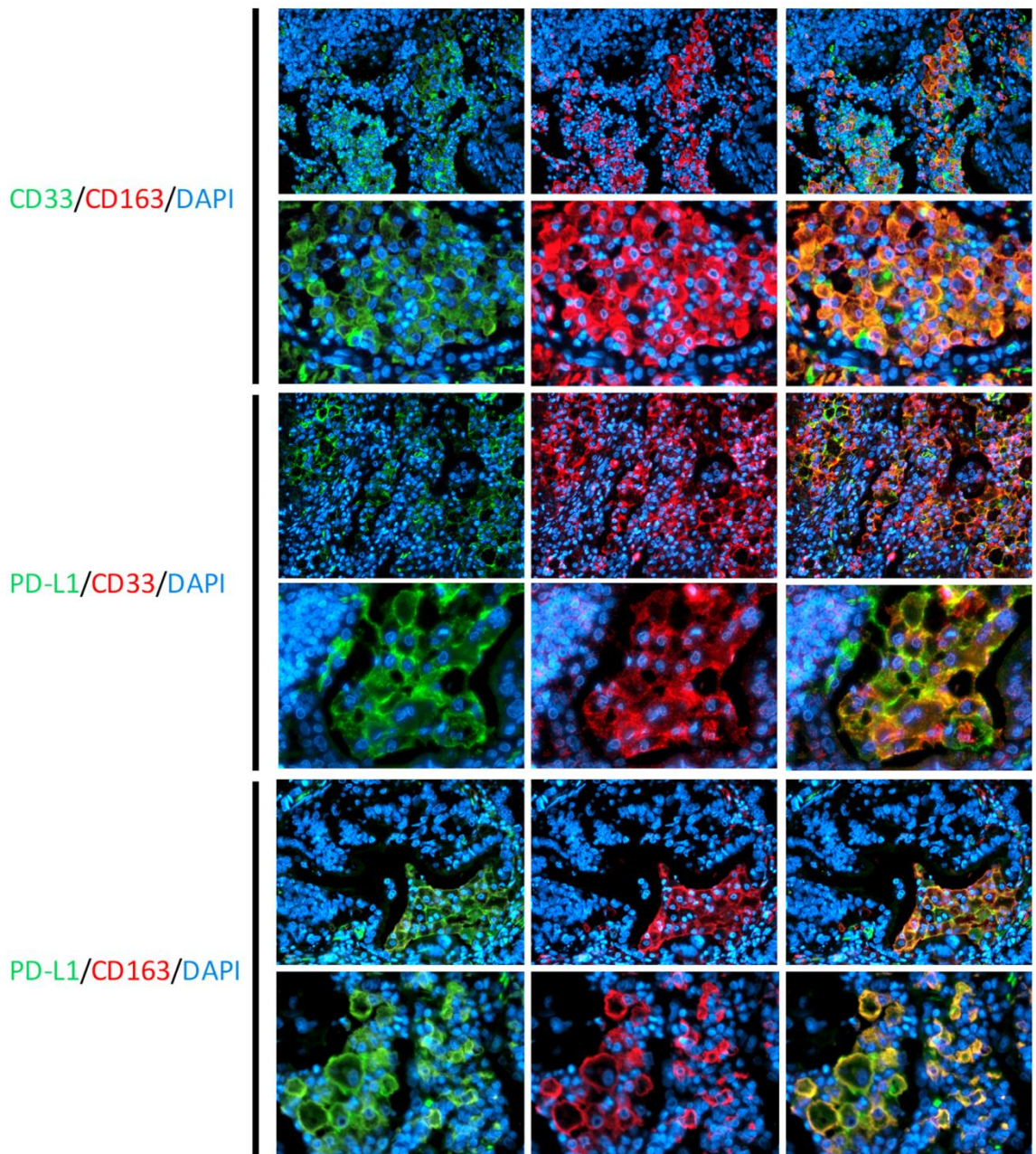
591   **determining HP**

592

27

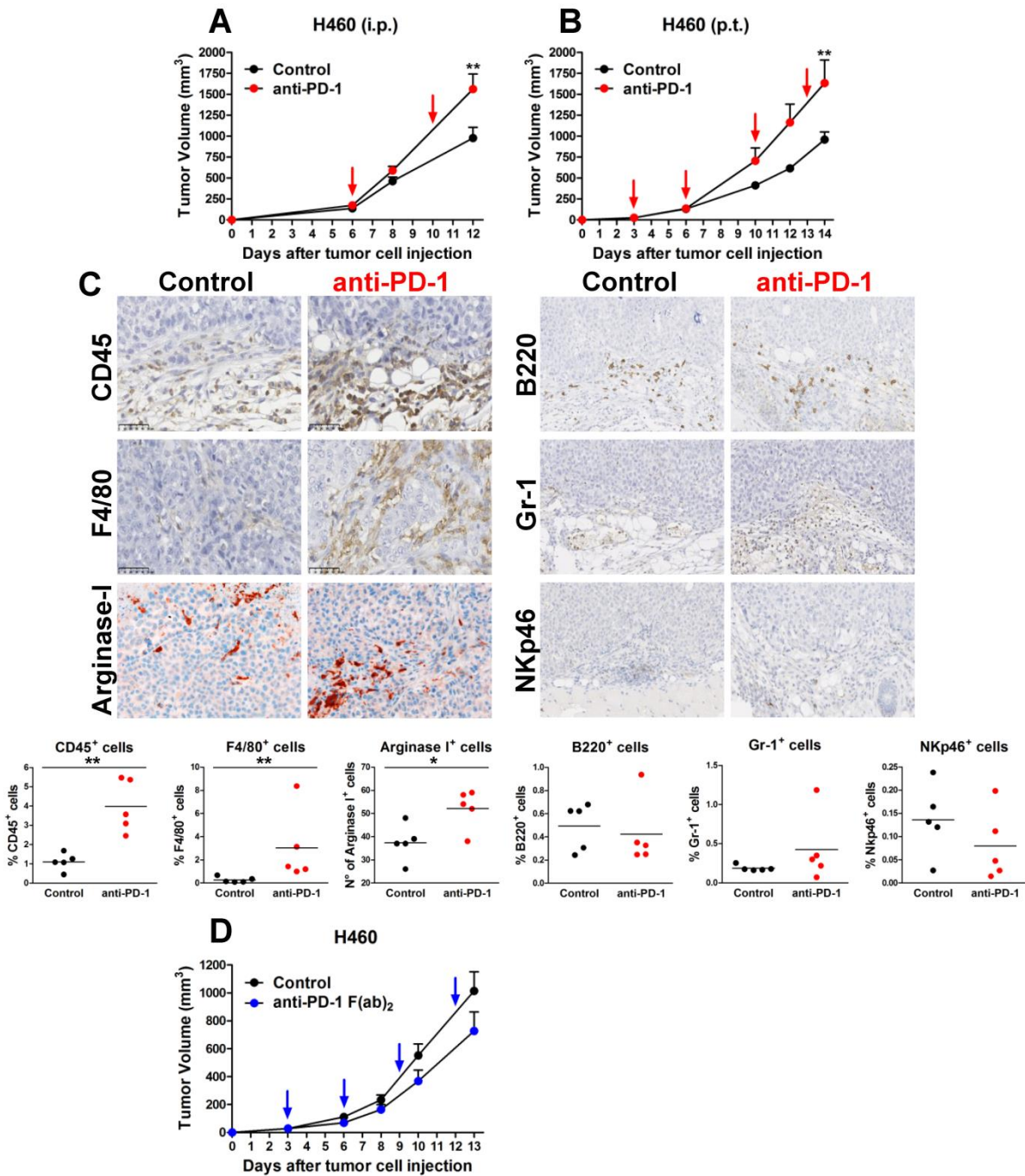**Figure 1**

CD33/CD163/DAPI

PD-L1/CD33/DAPI

PD-L1/CD163/DAPI

Figure2

Figure3
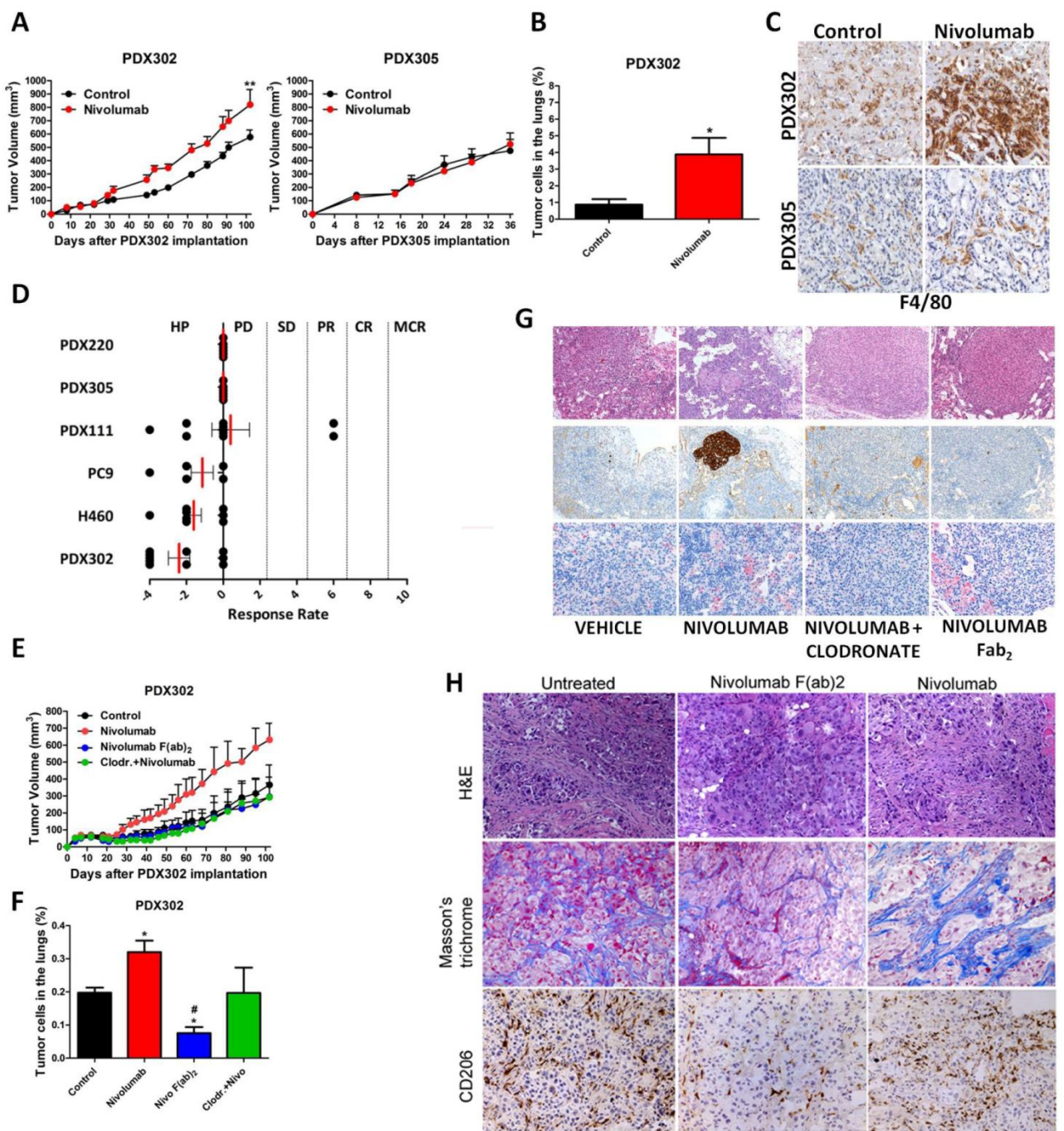
Figure 4
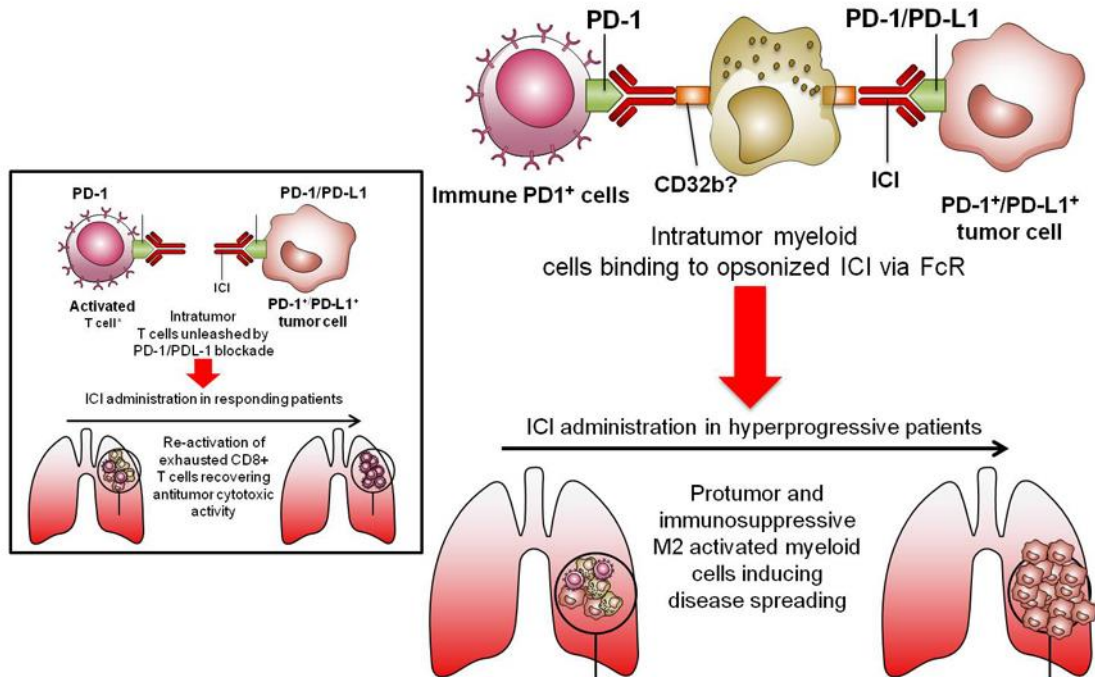
Figure5

AACR American Association for Cancer Research

Clinical Cancer Research

Antibody-Fc/FcR Interaction on Macrophages as a Mechanism for Hyperprogressive Disease in Non-Small Cell Lung Cancer Subsequent to PD-1/PD-L1 Blockade

Giuseppe Lo Russo, Massimo Moro, Michele Sommariva, et al.

Clin Cancer Res Published OnlineFirst September 11, 2018.

Updated version	Access the most recent version of this article at: doi:10.1158/1078-0432.CCR-18-1390
Supplementary Material	Access the most recent supplemental material at: http://clincancerres.aacrjournals.org/content/suppl/2018/09/11/1078-0432.CCR-18-1390.DC1
Author Manuscript	Author manuscripts have been peer reviewed and accepted for publication but have not yet been edited.

E-mail alerts	Sign up to receive free email-alerts related to this article or journal.
Reprints and Subscriptions	To order reprints of this article or to subscribe to the journal, contact the AACR Publications Department at pubs@aacr.org.
Permissions	To request permission to re-use all or part of this article, use this link http://clincancerres.aacrjournals.org/content/early/2018/09/11/1078-0432.CCR-18-1390. Click on "Request Permissions" which will take you to the Copyright Clearance Center's (CCC) Rightslink site.